

# Slepton pair production at the LHC in NLO+NLL with resummation-improved parton densities

---

Juri Fiaschi<sup>a</sup> and Michael Klasen<sup>a</sup>

<sup>a</sup>*Institut für Theoretische Physik, Westfälische Wilhelms-Universität Münster, Wilhelm-Klemm-Straße 9, D-48149 Münster, Germany*

*E-mail:* [fiaschi@uni-muenster.de](mailto:fiaschi@uni-muenster.de), [michael.klasen@uni-muenster.de](mailto:michael.klasen@uni-muenster.de)

**ABSTRACT:** Novel PDFs taking into account resummation-improved matrix elements, albeit only in the fit of a reduced data set, allow for consistent NLO+NLL calculations of slepton pair production at the LHC. We apply a factorisation method to this process that minimises the effect of the data set reduction, avoids the problem of outlier replicas in the NNPDF method for PDF uncertainties and preserves the reduction of the scale uncertainty. For Run II of the LHC, left-handed selectron/smuon, right-handed and maximally mixed stau production, we confirm that the consistent use of threshold-improved PDFs partially compensates the resummation contributions in the matrix elements. Together with the reduction of the scale uncertainty at NLO+NLL, the described method further increases the reliability of slepton pair production cross sections at the LHC.

**KEYWORDS:** Perturbative QCD, resummation, supersymmetry, hadron colliders

---

## Contents

<b>1</b>	<b>Introduction</b>	<b>1</b>
<b>2</b>	<b>Theoretical method</b>	<b>3</b>
<b>3</b>	<b>Left-handed selectron/smuon pair production</b>	<b>4</b>
<b>4</b>	<b>Right-handed and mixed stau pair production</b>	<b>7</b>
<b>5</b>	<b>Conclusion</b>	<b>9</b>

---

## 1 Introduction

Supersymmetry (SUSY) is a well-motivated extension of the Standard Model (SM) of particle physics that allows to answer simultaneously a significant number of its open questions [1, 2], but that can also be simplified in ways that can serve as prototypes for other, differently motivated models that address only a subset of these questions [3, 4]. Consequently, the search for SUSY particles continues to be an important research objective at the CERN LHC [5]. For the determination or exclusion of SUSY cross sections, particle masses and parameters [6], the experiments ATLAS and CMS rely on precise theoretical predictions in next-to-leading order (NLO) QCD [7–14] and beyond. In particular, threshold resummation techniques have been used successfully to take into account the emission of soft gluons and the associated leading, next-to-leading (NLL) and even next-to-next-to-leading logarithmic corrections to all orders in the strong coupling constant  $\alpha_s$ . These calculations have been performed for the production of squarks and gluinos [15–18], stops [19, 20], gauginos [21–26] and sleptons [27–31].

In our previous work on slepton pair production processes, we computed their NLO SUSY-QCD corrections [9] as well as NLL transverse-momentum [32], threshold [29] and joint [30] resummation corrections. These results are regularly applied to experimental analyses at the LHC [33–37]. We subsequently released the public code RESUMMINO [25], applied our results to simplified models and reanalysed public ATLAS and CMS data for various assumptions on the decomposition of the sleptons and their neutralino decay products [31].

The NLO+NLL corrections often increase the total SUSY particle production cross sections and therefore the experimental sensitivity with respect to NLO calculations. More importantly, they allow for a reduction of the theoretical uncertainty from the variation of the unphysical renormalisation and factorisation scales. While this could also be demonstrated in our previous work for slepton pair production, the second important theoretical uncertainty coming from the spread of parton density functions (PDFs) was not reduced,

as they were only determined by fitting data from deep-inelastic scattering (DIS), the Drell-Yan (DY) process, jet production etc. using NLO partonic matrix elements [38–40].

For consistency, hadronic cross sections should be computed with the same level of accuracy in both the partonic cross section and the PDFs. With the publication of the NNPDF30\_nll\_disdytop PDFs [41], this has now become possible at the NLO+NLL level. However, since only a reduced number of partonic cross sections that usually enter global fits are available with NLO+NLL precision, only a subset of the corresponding data sets, i.e. on DIS, DY and top pair production, could be used in the determination of these threshold-resummation improved PDFs. The consequence is that the PDF uncertainty band, produced with the NNPDF replica method, is actually larger, not smaller than with globally fitted NLO PDFs. One of the examples used in Ref. [41] is in fact slepton pair production, calculated with RESUMMINO. However, only one invariant-mass distribution for left-handed selectrons of mass 564 GeV is studied there.

The NNPDF30\_nll\_disdytop PDFs have subsequently been employed to investigate the effect of threshold-resummation improved PDFs on squark and gluino production [42]. The authors showed that the total central cross sections were modified both in a qualitative and quantitative way, illustrating the relevance and impact of using threshold-resummation improved PDFs. They introduced in particular a factorisation ( $K$ -factor) method, described in detail below, that allows to combine the impact of NLO+NLL threshold resummation on the reduced central PDF fit with the smaller uncertainty of the global NLO PDF fit, leading to approximately consistent NLO+NLL hadronic cross sections. This method also allows to avoid the problem of exceedingly large, small or even negative cross sections induced by outlier replicas and the lack of positivity constraints on the NNPDF PDFs. The replica method is known to be particularly problematic for resummation calculations, which rely on a transformation of PDFs to Mellin space from all regions of  $x$ , including those, where they are not well constrained [31].

The purpose of this paper is therefore threefold. First, our NLO+NLL predictions for slepton pair production are updated to the current LHC collision energy of 13 TeV. Second, we employ with NNPDF3.0 an up-to-date global set of PDFs, that is now also based on ATLAS and CMS data from jet, vector-boson and top-quark production [43]. This allows us to reach our third and central goal of studying the impact of threshold-resummation improved PDFs not only on differential, but also on total slepton pair production cross sections and for a variety of SUSY scenarios.

The remainder of this paper is organised as follows: In Sec. 2 we describe our theoretical approach using the  $K$ -factor method and how we combine NLO+NLL resummation effects with global PDF and also scale uncertainties. In Sec. 3, we present numerical results for differential and total cross sections of left-handed first and second generation sleptons in graphical and tabular form. We do this for  $pp$  collisions of 13 TeV centre-of-mass energy and various slepton masses relevant for Run II of the LHC. Similar results are presented in Sec. 4 for third-generation sleptons, i.e. right-handed or maximally mixed staus. Our conclusions are given in Sec. 5.

## 2 Theoretical method

Apart from updating our NLO+NLL predictions for slepton pair production to the current experimental conditions at Run II of the LHC, i.e. to proton-proton collisions with 13 TeV centre-of-mass energy, and with recent PDF sets from the global NNPDF3.0 fits, which are now also based on ATLAS and CMS data from jet, vector-boson and top-quark production [43], the central goal of this work is to quantify the impact of threshold-resummation improved PDFs on our predictions. These PDFs, called NNPDF30\_nll\_disdytop, have only recently been made available by the NNPDF collaboration [41]. They are based on a similar setup as those at leading order (LO) and NLO, but use partonic matrix elements at NLO+NLL, albeit so far only for a smaller set of processes (Deep-Inelastic Scattering, Drell-Yan and top-quark pair production), for which these matrix elements at NLO+NLL are available. Together with this NNPDF30\_nll\_disdytop fit, an NLO fit (NNPDF30\_nlo\_disdytop) based on the same subsample of processes and data sets has been provided. Unfortunately, the reduction of the input data set reduces the precision of these fits, and consequently they have currently still larger uncertainties than the global sets.

Threshold-resummation improved PDFs have previously been applied to squark and gluino production cross sections at NLO+NLL. The result there was that their effect cannot be neglected, as it modifies both the qualitative and the quantitative behaviour of the sparticle pair production cross sections [42]. In order to eliminate the impact of the reduction of the fitted data set, the authors introduced a  $K$ -factor

$$K = \frac{\sigma(\text{NLO} + \text{NLL})_{\text{NLO global}}}{\sigma(\text{NLO})_{\text{NLO global}}} \cdot \frac{\sigma(\text{NLO} + \text{NLL})_{\text{NLO+NLL reduced}}}{\sigma(\text{NLO} + \text{NLL})_{\text{NLO reduced}}}, \quad (2.1)$$

which allows to obtain (approximate) central total NLO+NLL cross sections with NLO+NLL PDFs via

$$\sigma(\text{NLO} + \text{NLL})_{\text{NLL+NLO global}} = K \cdot \sigma(\text{NLO})_{\text{NLO global}}. \quad (2.2)$$

Varying the NLO global PDFs in  $\sigma(\text{NLO})_{\text{NLO global}}$  with their reliable spread then produces a reliable (approximate) NLO+NLL global PDF error. In Eq. (2.1), the first ratio takes into account the effect of the resummation in the partonic matrix elements using the NLO PDF fit of the global data set, whereas the second ratio parameterises the impact of the threshold-resummation improved partonic matrix elements on the NLO+NLL PDF fit of the reduced data set. As explained above, we use the NLO global NNPDF3.0 PDF set [43] for the computation of the first ratio related to the global part, while the NLO+NLL and NLO PDF fits based on the reduced data set [41] enter the evaluation of the second ratio. A definition equivalent to Eq. (2.2) is adopted for invariant-mass distributions by simply replacing the total integrated cross section  $\sigma$  with the differential cross sections  $d\sigma/dM_{\tilde{\ell}\tilde{\ell}}$ .

With the method described above, we also bypass a known issue with the NNPDF approach to PDF uncertainties. In order to compute this systematic error, the NNPDF collaboration fit a large number of Gaussian-distributed replicas of the experimental data without imposing ad-hoc conditions on the shape or positivity of the PDFs to avoid theoretical bias or underestimation of the resulting PDF uncertainty. The PDF uncertainty on

any observable results from applying to it the ensemble of the replica fits. However, positivity is and practically can be checked only for a subset of observables. The complication encountered in resummation calculations is that the PDF replicas have to be transformed to Mellin space, i.e. be integrated over regions in  $x$  where they are not well constrained, which can then lead to unphysically large variations of the resummed cross sections [31]. At NLO and in  $x$ -space, one can directly eliminate the replicas that feature such misbehaviour [43]. Alternatively, one can consider only the 68% CL interval by eliminating the replicas leading to the lowest and highest 16 cross sections, respectively, and use the midpoint of this interval as the central prediction [44]. Note that this prescription leads to central predictions that differ substantially from those obtained with the central PDF fit. The  $K$ -factor method described above provides a more elegant solution to the problem of outlier replicas entering resummation predictions by avoiding their transformation to Mellin space altogether. According to Eq. (2.1) only the NLO global, NLO reduced and NLO+NLL reduced central fits have to be transformed, and according to Eq. (2.2) the global replicas have to be applied only at NLO and in  $x$ -space.

The  $K$ -factor method conceals one important benefit of the resummation calculation, which is the sizeable reduction of scale uncertainties. This reduction from NLO to NLO+NLL would be lost if the scales were varied only in the NLO cross section in Eq. (2.2) with respect to the central scale  $\mu_R = \mu_F = m_{\tilde{\ell}}$ . It is therefore evaluated directly in the NLO+NLL (or NLO) cross sections by applying the usual seven-point method of relative factors of two, but not four among the two types of scales. The total theoretical uncertainty is then obtained by adding the relative PDF and scale uncertainties in quadrature.

### 3 Left-handed selectron/smuon pair production

In this section, we study the effects of the threshold-improved NLO+NLL PDFs as implemented in LHAPDF6 [45] on invariant-mass distributions and total cross sections for left-handed first- and second-generation slepton pair production using RESUMMINO [25]. If we assume as usual universality of the corresponding soft SUSY-breaking masses and do not take into account branching ratios and experimental efficiencies, selectron and smuon production cross sections are identical. We set all SM parameters to their current PDG values [46] and use  $\alpha_s(M_Z) = 0.118$  with  $\Lambda_{n_f=5}^{\overline{\text{MS}}} = 0.239$  GeV as appropriate for NNPDF3.0.

In the upper panel of Fig. 1, we show the invariant-mass distribution of left-handed selectron/smuon pairs with a fixed mass of  $m_{\tilde{\ell}} = 564$  GeV. This mass is identical to the one chosen in Ref. [41] in order to facilitate a straightforward comparison of our results. The invariant mass distributions, computed at LO (dotted green), NLO (dashed blue) and NLO+NLL (full red line) in the matrix elements, but always with global NLO NNPDF3.0 PDFs, exhibit the typical rise above pair production threshold to about  $M_{\tilde{\ell}\tilde{\ell}} = 1.4$  TeV and a subsequent fall-off. At the maximum, an increase of about 16% is visible from LO to NLO with an increase of another 2% from NLO to NLO+NLL, which then rises to 3% at  $M_{\tilde{\ell}\tilde{\ell}} = 3$  TeV as expected.

The lower panel of Fig. 1 shows the  $K$ -factor as defined in Eq. (2.1) (full red) as well as its second part (dashed blue line) that comes from the change of PDFs alone. The

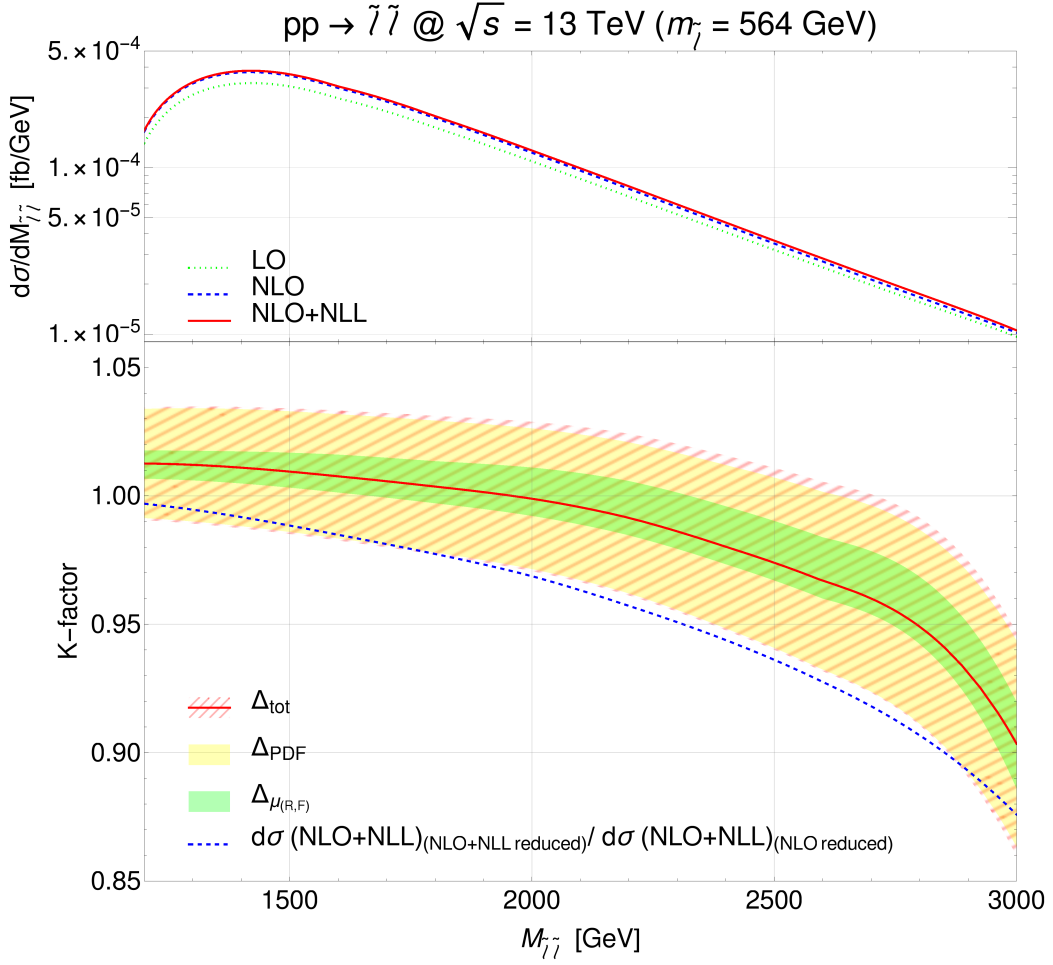


**Figure 1.** Invariant-mass distributions (upper panel) and  $K$ -factors (lower panel) according to Eq. (2.1) using the full expression (full red) and only its second, PDF-dependent part (dashed blue line) for the pair production of left-handed selectrons/smuons with a mass of  $m_{\tilde{\ell}} = 564$  GeV at the LHC with  $\sqrt{s} = 13$  TeV. In the upper panel, the results at LO (dotted green), NLO (dashed blue) and NLO+NLL (full red line) have been obtained with global NLO PDFs. In the lower panel, the PDF (yellow) and scale (green) uncertainties have been computed at NLO and NLO+NLL, respectively, with global NLO PDFs, then rescaled appropriately and added in quadrature for the total theoretical uncertainty (dashed red).

latter amounts to a decrease of more than 10% at high invariant mass, which is partially compensated by the NLL corrections in the matrix elements. At low invariant mass, one observes even an overcompensation, such that the total  $K$ -factor is slightly larger than unity. This effect was also observed in Fig. 17 of Ref. [41]. Our results agree quite well with theirs despite the fact that they show the slightly different factor

$$K' = \frac{\sigma(\text{NLO} + \text{NLL})_{\text{NLO+NLL reduced}}}{\sigma(\text{NLO})_{\text{NLO global}}}. \quad (3.1)$$

This  $K'$ -factor thus also includes the impact of the reduction of the data set in the PDF fits from NLO to NLO+NLL, which we preferred to remove from our analysis and which impacts mostly the region of large invariant mass or parton momentum fraction, where the PDFs are not well constrained. A second difference in our figure is our (yellow) PDF uncertainty band, which is based on the more reliable global NLO fit, while the (dashed red) band in Ref. [41] is based on the reduced data set and thus considerably larger. Furthermore, we also show the (green) scale uncertainty obtained with the usual seven-point method, which, as expected from the reduction due to NLL resummation contributions, contributes only little to the total (dashed red) uncertainty (added in quadrature). Remember that the scale uncertainty has been computed directly at NLO+NLL using the global NLO PDFs and has then been rescaled appropriately (cf. Sec. 2).

To estimate the size of (N)NNLL over NLL threshold resummation effects in both the matrix elements and the PDFs, it is instructive to compare the invariant mass distributions for slepton pairs in the lower right plot of Fig. 7 of Ref. [28] and of the quark-antiquark luminosities in the upper left plots of Figs. 13 and 14 of Ref. [41]. While the former lie at the upper end of the NLL uncertainty band, the latter are reduced by 1-2% with respect to NLL, confirming again further increased perturbative stability and additional partial compensation of resummation effects in the PDFs.

In Fig. 2 we show similar results, but now for the total cross section as a function of the selectron/smuon mass. As can be seen in the upper panel, left-handed sleptons should have been produced in significant numbers already at Run II of the LHC with luminosities recorded in 2016-2017 by ATLAS and CMS of  $35\text{-}50\text{ fb}^{-1}$  each over most of the mass region shown. Indeed, current left- (right-) handed slepton mass limits reach values of 400 (290) GeV, but they depend strongly on the mass splitting with the lightest SUSY particle, usually assumed to be the lightest neutralino  $\tilde{\chi}_1^0$  [34, 37].

The central  $K$ -factor (full red line) in the lower panel shows that the NLO+NLL PDFs reduce not only the invariant-mass distribution, but also the total cross section by up to 4% for large slepton masses, where their effect partially compensates again the impact of the NLL corrections in the matrix elements. This result agrees with the one for squark pair production in Fig. 8 and with the result for the underlying quark-quark luminosity in Fig. 7 of Ref. [42]. The difference with the quark-antiquark luminosity is of minor importance in the sea-quark region. For large slepton masses, the total  $K$ -factor from NLO to NLO+NLL is not only larger than the scale, but also the PDF uncertainty. In contrast, the impact of the NLO+NLL matrix elements on the PDF fit alone falls within this uncertainty.

We conclude this section for future use, e.g. by the LHC experiments, with explicit results in Tab. 1 on the total cross sections at LO, NLO and NLO+NLL, that have been obtained with consistent PDF choices using Eq. (2.2), and on the corresponding theoretical uncertainties. The central NLO+NLL results have been obtained with the  $K$ -factor method, while the NLO+NLL (asymmetric) scale uncertainties have been computed directly, and the PDF (symmetric) uncertainties at NLO. The latter are therefore identical in the last two columns.



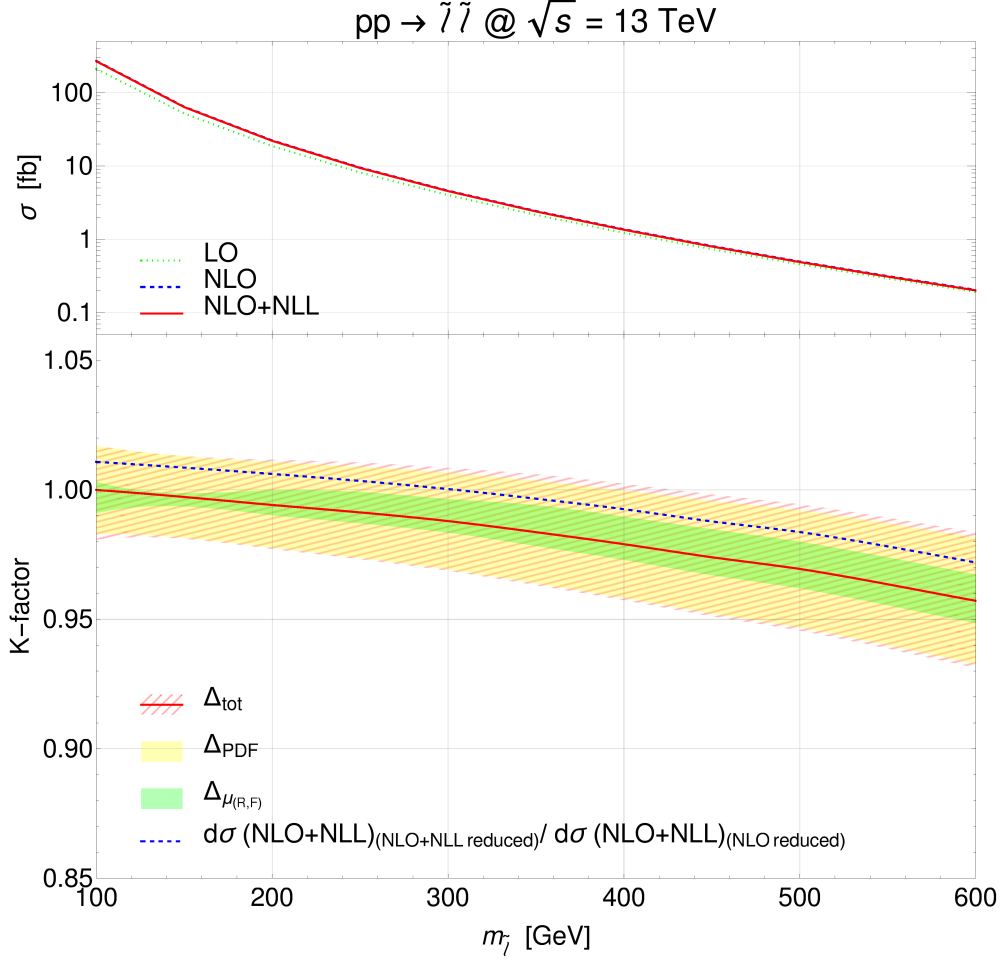


**Figure 2.** Same as Fig. 1, but for the total cross section as a function of the selectron/smudon mass.

#### 4 Right-handed and mixed stau pair production

In this section we repeat the analysis of Sec. 3 for right-handed and maximally mixed stau pair production. Since the off-diagonal elements of the sfermion mixing matrices are proportional to the SM fermion mass, mixing of chirality superpartners is only important for third-generation sfermions, i.e. in our case for tau sleptons. At the cross section level, left-handed stau cross sections are identical to those for selectrons and smuons, so that we do not show the corresponding results again. Experimentally, the analysis for staus is, of course, very different, since their decay products are unstable tau leptons, that are not directly measured in the tracking systems, electromagnetic calorimeters or muon chambers, but that have to be reconstructed themselves from hadronic [47, 48] and/or leptonic [36] decay products.

In the upper panels of Fig. 3 we show the total cross sections for right-handed (left) and maximally mixed (right) stau pairs computed at LO (dotted green), NLO (dashed blue)



**Table 1.** Total cross section for first-generation slepton pair production at the LHC with  $\sqrt{s} = 13$  TeV as a function of the slepton mass at LO, NLO and NLO+NLL with consistent PDF choices. The central NLO+NLL results are obtained with the  $K$ -factor method, whereas the NLO+NLL (asymmetric) scale uncertainty has been computed directly, and the PDF (symmetric) uncertainty at NLO (identical in the last two columns).

$m_{\tilde{\ell}}$ [GeV]	LO (LO global) [fb]	NLO (NLO global) [fb]	NLO+NLL (id. global) [fb]
100	$210.40^{+3.5\%}_{-4.4\%} \pm 7.6\%$	$271.24^{+2.1\%}_{-1.7\%} \pm 1.7\%$	$271.22^{+0.3\%}_{-0.9\%} \pm 1.7\%$
150	$52.16^{+0.6\%}_{-1.2\%} \pm 6.3\%$	$64.23^{+2.1\%}_{-1.4\%} \pm 1.6\%$	$64.05^{+0.2\%}_{-0.4\%} \pm 1.6\%$
200	$18.68^{+0.8\%}_{-1.1\%} \pm 6.2\%$	$22.32^{+2.1\%}_{-1.5\%} \pm 1.7\%$	$22.19^{+0.6\%}_{-0.4\%} \pm 1.7\%$
250	$8.14^{+2.2\%}_{-2.4\%} \pm 6.2\%$	$9.51^{+2.2\%}_{-1.6\%} \pm 1.8\%$	$9.42^{+0.8\%}_{-0.4\%} \pm 1.8\%$
300	$4.01^{+3.4\%}_{-3.3\%} \pm 6.2\%$	$4.60^{+2.1\%}_{-1.8\%} \pm 1.9\%$	$4.55^{+0.9\%}_{-0.5\%} \pm 1.9\%$
350	$2.15^{+4.3\%}_{-4.1\%} \pm 6.2\%$	$2.43^{+2.1\%}_{-2.0\%} \pm 2.0\%$	$2.39^{+1.1\%}_{-0.5\%} \pm 2.0\%$
400	$1.23^{+5.1\%}_{-4.8\%} \pm 6.2\%$	$1.37^{+2.1\%}_{-2.1\%} \pm 2.1\%$	$1.34^{+1.1\%}_{-0.6\%} \pm 2.1\%$
450	$0.74^{+5.8\%}_{-5.3\%} \pm 6.3\%$	$0.81^{+2.1\%}_{-2.2\%} \pm 2.2\%$	$0.79^{+1.1\%}_{-0.7\%} \pm 2.2\%$
500	$0.46^{+6.5\%}_{-5.8\%} \pm 6.4\%$	$0.50^{+2.1\%}_{-2.3\%} \pm 2.3\%$	$0.48^{+1.1\%}_{-0.8\%} \pm 2.3\%$
550	$0.29^{+7.0\%}_{-6.3\%} \pm 6.5\%$	$0.31^{+2.1\%}_{-2.4\%} \pm 2.4\%$	$0.30^{+1.1\%}_{-0.8\%} \pm 2.4\%$
600	$0.19^{+7.5\%}_{-6.7\%} \pm 6.7\%$	$0.20^{+2.2\%}_{-2.6\%} \pm 2.6\%$	$0.20^{+1.1\%}_{-0.9\%} \pm 2.6\%$

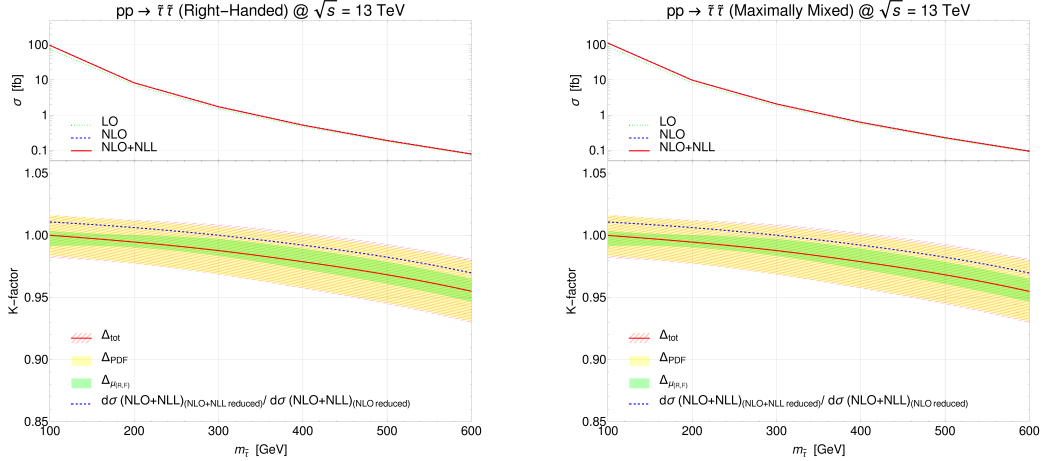


**Figure 3.** Same as Fig. 2, but for the pair production of right-handed (left) and maximally mixed (right) staus.

and NLO+NLL (full red line) with global NLO PDFs. We follow here the experimental analysis in Ref. [48] and extend it from masses of 400 GeV to 600 GeV. The total cross sections for right-handed staus are clearly smaller than those for left-handed sleptons in Fig. 2, with those for maximally mixed staus lying between the two extremes. Compared to the cross sections in Run I of the LHC at  $\sqrt{s} = 7$  TeV (8 TeV) as listed in Tab. 1 (2) of Ref. [31], they are increased by a factor of 2.5 (2) at low slepton masses and up to a

**Table 2.** Same as Tab. 1, but for the pair production of right-handed staus.

$m_{\tilde{\tau}}$ [GeV]	LO (LO global) [fb]	NLO (NLO global) [fb]	NLO+NLL (id. global) [fb]
100	$75.68^{+3.4\%}_{-4.3\%} \pm 6.4\%$	$97.19^{+2.1\%}_{-1.7\%} \pm 1.6\%$	$97.20^{+0.4\%}_{-0.9\%} \pm 1.6\%$
200	$7.03^{+0.8\%}_{-1.1\%} \pm 6.2\%$	$8.37^{+2.2\%}_{-1.5\%} \pm 1.7\%$	$8.33^{+0.6\%}_{-0.4\%} \pm 1.7\%$
300	$1.53^{+3.3\%}_{-3.3\%} \pm 6.2\%$	$1.75^{+2.1\%}_{-1.8\%} \pm 1.9\%$	$1.73^{+0.9\%}_{-0.4\%} \pm 1.9\%$
400	$0.47^{+5.1\%}_{-4.7\%} \pm 6.2\%$	$0.53^{+2.1\%}_{-2.1\%} \pm 2.1\%$	$0.51^{+1.1\%}_{-0.6\%} \pm 2.1\%$
500	$0.18^{+6.4\%}_{-5.8\%} \pm 6.3\%$	$0.19^{+2.1\%}_{-2.3\%} \pm 2.3\%$	$0.19^{+1.1\%}_{-0.8\%} \pm 2.3\%$
600	$0.075^{+7.4\%}_{-6.6\%} \pm 6.6\%$	$0.080^{+2.2\%}_{-2.5\%} \pm 2.5\%$	$0.076^{+1.1\%}_{-0.9\%} \pm 2.5\%$

factor of 10 (5) at high slepton masses. The PDF update from the NLO fit of CT10 [38] used in Ref. [31] to the global NLO fit of NNPDF3.0 used here changes the NLO+NLL cross sections insignificantly at low slepton masses and by up to 5% at high slepton masses, which fell well into the CT10 PDF uncertainty, but exceeds the current NNPDF3.0 PDF uncertainty. Although the total cross sections are relatively large over the full mass range shown and should have led to the production of staus in significant numbers at the LHC, only upper limits on the cross sections could so far be derived by ATLAS in Run I [47] and by CMS in Run II [48] in the purely hadronic decay channel and by CMS, for left-handed staus, in the (semi-)leptonic decay channel(s) [36].

The lower panels of Fig. 3 show the corresponding  $K$ -factors according to the full expression of Eq. (2.1) (full red) and to its second, PDF-dependent part only (dashed blue line), together with the PDF (yellow), scale (green) and total theoretical uncertainty (dashed red). The QCD corrections turn out to be largely independent of the weak coupling structure of the underlying partonic cross section, so that the dependence on the weak couplings cancels in the ratios and no differences are visible in the  $K$ -factors with respect to those of first-generation left-handed sleptons in the lower panel of Fig. 3.

For better readability and future use, we end this section by listing consistent total cross sections for right-handed and maximally mixed stau pair production at LO, NLO and NLO+NLL in Tabs. 2 and 3. The central NLO+NLL results have again been obtained with the  $K$ -factor method, while the NLO+NLL (asymmetric) scale uncertainties have been computed directly, and the PDF (symmetric) uncertainties at NLO using the global NNPDF3.0 fits. The latter are therefore again identical in the last two columns.

## 5 Conclusion

To summarise, we have studied in this paper the effect of modern, NLO+NLL PDFs on consistent NLO+NLL predictions for slepton pair production at Run II of the LHC. Compared to previous work by us and other authors, we have updated the analysis of left-handed selectron or smuon as well as right-handed and maximally mixed stau pair production to the current LHC centre-of-mass energy of 13 TeV. Also, cross sections at LO, NLO and NLO+NLL have been computed with NNPDF3.0 PDFs from a global fit

**Table 3.** Same as Tab. 1, but for the pair production of maximally mixed staus.

$m_{\tilde{\tau}}$ [GeV]	LO (LO global) [fb]	NLO (NLO global) [fb]	NLO+NLL (id. global) [fb]
100	$87.99^{+3.3\%}_{-4.2\%} \pm 6.4\%$	$112.83^{+2.1\%}_{-1.7\%} \pm 1.6\%$	$112.82^{+0.3\%}_{-0.9\%} \pm 1.6\%$
200	$8.40^{+0.8\%}_{-1.1\%} \pm 6.2\%$	$9.99^{+2.2\%}_{-1.5\%} \pm 1.7\%$	$9.94^{+0.6\%}_{-0.4\%} \pm 1.7\%$
300	$1.84^{+3.3\%}_{-3.3\%} \pm 6.2\%$	$2.10^{+2.1\%}_{-1.8\%} \pm 1.9\%$	$2.07^{+0.9\%}_{-0.4\%} \pm 1.9\%$
400	$0.57^{+5.1\%}_{-4.7\%} \pm 6.2\%$	$0.63^{+2.1\%}_{-2.1\%} \pm 2.1\%$	$0.62^{+1.1\%}_{-0.6\%} \pm 2.1\%$
500	$0.21^{+6.4\%}_{-5.8\%} \pm 6.3\%$	$0.23^{+2.1\%}_{-2.3\%} \pm 2.3\%$	$0.22^{+1.1\%}_{-0.8\%} \pm 2.3\%$
600	$0.090^{+7.4\%}_{-6.6\%} \pm 6.6\%$	$0.096^{+2.2\%}_{-2.5\%} \pm 2.5\%$	$0.091^{+1.1\%}_{-0.9\%} \pm 2.5\%$

at NLO and their uncertainties as estimated with the replica method, as well as from a fit based on threshold-resummation improved NLO+NLL matrix elements of a reduced set of observables (DIS, DY and top pair production). We applied a factorisation method proposed previously that minimises the effect of the data set reduction in the PDF fits, avoids the known problem of outlier replicas, and preserves the reduction of the scale uncertainty in our resummation calculation.

Apart from the generally known fact that hadronic cross sections increase significantly at higher collision energies, we also observed slightly larger cross sections, in particular for large slepton masses, due to the NLO PDF update. We confirmed that the consistent use of threshold-improved PDFs partially compensates resummation contributions in the matrix elements. Together with the reduced scale uncertainty at NLO+NLL, the described method further increases the reliability of slepton pair production cross sections at the LHC. The new method has been implemented for sleptons in the public code RESUMMINO.

## Acknowledgements

We thank Marco Bonvini for useful discussions about the NNPDF3.0 resummation-improved PDFs. We also thank Valentina Dutta for providing us with the parameter cards used for the CMS stau mixing scenarios and Pieter Everaerts for the punctual clarifications about the CMS stau analysis. This work has been supported by the BMBF under contract 05H15PMCCA and the DFG through the Research Training Network 2149 “Strong and weak interactions - from hadrons to dark matter”.

## References

- [1] H. P. Nilles, [Phys. Rept. \*\*110\*\*, 1 \(1984\)](#).
- [2] H. E. Haber and G. L. Kane, [Phys. Rept. \*\*117\*\*, 75 \(1985\)](#).
- [3] J. Alwall, P. Schuster, and N. Toro, [Phys. Rev. \*\*D79\*\*, 075020 \(2009\)](#), [arXiv:0810.3921 \[hep-ph\]](#).
- [4] L. Calibbi, J. M. Lindert, T. Ota, and Y. Takanishi, [JHEP \*\*11\*\*, 106 \(2014\)](#), [arXiv:1410.5730 \[hep-ph\]](#).

- [5] F. Giordano (ATLAS, CMS), *Proceedings, 15th Incontri di Fisica delle Alte Energie (IFAE 2016): Genoa, Italy, March 30-April 1, 2016*, *Nuovo Cim.* **C40**, 2 (2017).
- [6] J. A. Aguilar-Saavedra *et al.*, *Eur. Phys. J.* **C46**, 43 (2006), [arXiv:hep-ph/0511344 \[hep-ph\]](#) .
- [7] W. Beenakker, R. Hopker, M. Spira, and P. M. Zerwas, *Nucl. Phys.* **B492**, 51 (1997), [arXiv:hep-ph/9610490 \[hep-ph\]](#) .
- [8] W. Beenakker, M. Kramer, T. Plehn, M. Spira, and P. M. Zerwas, *Nucl. Phys.* **B515**, 3 (1998), [arXiv:hep-ph/9710451 \[hep-ph\]](#) .
- [9] W. Beenakker, M. Klasen, M. Kramer, T. Plehn, M. Spira, and P. M. Zerwas, *Phys. Rev. Lett.* **83**, 3780 (1999), [Erratum: *Phys. Rev. Lett.* 100, 029901 (2008)], [arXiv:hep-ph/9906298 \[hep-ph\]](#) .
- [10] E. L. Berger, M. Klasen, and T. M. P. Tait, *Phys. Lett.* **B459**, 165 (1999), [arXiv:hep-ph/9902350 \[hep-ph\]](#) .
- [11] E. L. Berger, M. Klasen, and T. M. P. Tait, *Phys. Rev.* **D62**, 095014 (2000), [Erratum: *Phys. Rev.* D67, 099901 (2003)], [arXiv:hep-ph/0212306 \[hep-ph\]](#) .
- [12] M. Spira, in *Supersymmetry and unification of fundamental interactions. Proceedings, 10th International Conference, SUSY'02, Hamburg, Germany, June 17-23, 2002* (2002) pp. 217–226, [arXiv:hep-ph/0211145 \[hep-ph\]](#) .
- [13] L. G. Jin, C. S. Li, and J. J. Liu, *Phys. Lett.* **B561**, 135 (2003), [arXiv:hep-ph/0307390 \[hep-ph\]](#) .
- [14] T. Binoth, D. Goncalves Netto, D. Lopez-Val, K. Mawatari, T. Plehn, and I. Wigmore, *Phys. Rev.* **D84**, 075005 (2011), [arXiv:1108.1250 \[hep-ph\]](#) .
- [15] W. Beenakker, C. Borschensky, M. Kramer, A. Kulesza, E. Laenen, V. Theeuwes, and S. Thewes, *JHEP* **12**, 023 (2014), [arXiv:1404.3134 \[hep-ph\]](#) .
- [16] C. Borschensky, M. Kramer, A. Kulesza, M. Mangano, S. Padhi, T. Plehn, and X. Portell, *Eur. Phys. J.* **C74**, 3174 (2014), [arXiv:1407.5066 \[hep-ph\]](#) .
- [17] M. Beneke, J. Piclum, C. Schwinn, and C. Wever, *JHEP* **10**, 054 (2016), [arXiv:1607.07574 \[hep-ph\]](#) .
- [18] W. Beenakker, C. Borschensky, M. Kramer, A. Kulesza, and E. Laenen, *JHEP* **12**, 133 (2016), [arXiv:1607.07741 \[hep-ph\]](#) .
- [19] A. Broggio, A. Ferroglia, M. Neubert, L. Vernazza, and L. L. Yang, *JHEP* **03**, 066 (2014), [arXiv:1312.4540 \[hep-ph\]](#) .
- [20] W. Beenakker, C. Borschensky, R. Heger, M. Kramer, A. Kulesza, and E. Laenen, *JHEP* **05**, 153 (2016), [arXiv:1601.02954 \[hep-ph\]](#) .
- [21] C. S. Li, Z. Li, R. J. Oakes, and L. L. Yang, *Phys. Rev.* **D77**, 034010 (2008), [arXiv:0707.3952 \[hep-ph\]](#) .
- [22] J. Debove, B. Fuks, and M. Klasen, *Nucl. Phys.* **B842**, 51 (2011), [arXiv:1005.2909 \[hep-ph\]](#) .
- [23] J. Debove, B. Fuks, and M. Klasen, *Nucl. Phys.* **B849**, 64 (2011), [arXiv:1102.4422 \[hep-ph\]](#) .
- [24] B. Fuks, M. Klasen, D. R. Lamprea, and M. Rothering, *JHEP* **10**, 081 (2012), [arXiv:1207.2159 \[hep-ph\]](#) .
- [25] B. Fuks, M. Klasen, D. R. Lamprea, and M. Rothering, *Eur. Phys. J.* **C73**, 2480 (2013), [arXiv:1304.0790 \[hep-ph\]](#) .

- [26] B. Fuks, M. Klasen, and M. Rothering, *JHEP* **07**, 053 (2016), [arXiv:1604.01023 \[hep-ph\]](#) .
- [27] L. L. Yang, C. S. Li, J. J. Liu, and Q. Li, *Phys. Rev.* **D72**, 074026 (2005), [arXiv:hep-ph/0507331 \[hep-ph\]](#) .
- [28] A. Broggio, M. Neubert, and L. Vernazza, *JHEP* **05**, 151 (2012), [arXiv:1111.6624 \[hep-ph\]](#) .
- [29] G. Bozzi, B. Fuks, and M. Klasen, *Nucl. Phys.* **B777**, 157 (2007), [arXiv:hep-ph/0701202 \[hep-ph\]](#) .
- [30] G. Bozzi, B. Fuks, and M. Klasen, *Nucl. Phys.* **B794**, 46 (2008), [arXiv:0709.3057 \[hep-ph\]](#) .
- [31] B. Fuks, M. Klasen, D. R. Lamprea, and M. Rothering, *JHEP* **01**, 168 (2014), [arXiv:1310.2621](#) .
- [32] G. Bozzi, B. Fuks, and M. Klasen, *Phys. Rev.* **D74**, 015001 (2006), [arXiv:hep-ph/0603074 \[hep-ph\]](#) .
- [33] G. Aad *et al.* (ATLAS), *Phys. Rev.* **D93**, 052002 (2016), [arXiv:1509.07152 \[hep-ex\]](#) .
- [34] M. Aaboud *et al.* (ATLAS), (2017), [arXiv:1712.08119 \[hep-ex\]](#) .
- [35] V. Khachatryan *et al.* (CMS), *Eur. Phys. J.* **C74**, 3036 (2014), [arXiv:1405.7570 \[hep-ex\]](#) .
- [36] V. Khachatryan *et al.* (CMS), CMS-PAS-SUS-17-002 (2017).
- [37] V. Khachatryan *et al.* (CMS), CMS-PAS-SUS-17-009 (2017).
- [38] H.-L. Lai, M. Guzzi, J. Huston, Z. Li, P. M. Nadolsky, J. Pumplin, and C. P. Yuan, *Phys. Rev.* **D82**, 074024 (2010), [arXiv:1007.2241 \[hep-ph\]](#) .
- [39] A. D. Martin, W. J. Stirling, R. S. Thorne, and G. Watt, *Eur. Phys. J.* **C63**, 189 (2009), [arXiv:0901.0002 \[hep-ph\]](#) .
- [40] R. D. Ball, V. Bertone, S. Carrazza, L. Del Debbio, S. Forte, A. Guffanti, N. P. Hartland, and J. Rojo (NNPDF), *Nucl. Phys.* **B877**, 290 (2013), [arXiv:1308.0598 \[hep-ph\]](#) .
- [41] M. Bonvini, S. Marzani, J. Rojo, L. Rottoli, M. Ubiali, R. D. Ball, V. Bertone, S. Carrazza, and N. P. Hartland, *JHEP* **09**, 191 (2015), [arXiv:1507.01006 \[hep-ph\]](#) .
- [42] W. Beenakker, C. Borschensky, M. Kramer, A. Kulesza, E. Laenen, S. Marzani, and J. Rojo, *Eur. Phys. J.* **C76**, 53 (2016), [arXiv:1510.00375 \[hep-ph\]](#) .
- [43] R. D. Ball *et al.* (NNPDF), *JHEP* **04**, 040 (2015), [arXiv:1410.8849 \[hep-ph\]](#) .
- [44] J. Butterworth *et al.*, *J. Phys.* **G43**, 023001 (2016), [arXiv:1510.03865 \[hep-ph\]](#) .
- [45] A. Buckley, J. Ferrando, S. Lloyd, K. Nordstrom, B. Page, M. Rufenacht, M. Schonherr, and G. Watt, *Eur. Phys. J.* **C75**, 132 (2015), [arXiv:1412.7420 \[hep-ph\]](#) .
- [46] C. Patrignani *et al.* (Particle Data Group), *Chin. Phys.* **C40**, 100001 (2016).
- [47] G. Aad *et al.* (ATLAS), *JHEP* **10**, 096 (2014), [arXiv:1407.0350 \[hep-ex\]](#) .
- [48] V. Khachatryan *et al.* (CMS), CMS-PAS-SUS-17-003 (2017).